JOURNAL OF MATERIALS SCIENCE **37** (2002) 1813–1821

Processing and microstructural characterization of functionally gradient Al A359/SiC_p composite

R. RODRIGUEZ-CASTRO
Instituto Tecnológico de Celaya, Departamento de Ingeniería Mecánica, 38010 Celaya, Gto., Mexico

M. H. KELESTEMUR*
Firat University, School of Engineering, Metallurgy and Material Science Department, Elazig, Turkey
E-mail: hkelestemur@firat.edu.tr

A centrifugal casting method is presented in this paper for processing Al/SiC_p Functionally Gradient Material (FGM), along with the corresponding microstructural characterization. Results are presented and discussed on SiC particles distribution, particles-solidification front interactions, matrix micro-structure, and porosity distribution in the castings as a function of the centrifugal forces applied. Three different casting rotational speeds (700, 1000 and 1300 rpm) were utilized while keeping all other casting conditions constant. For the highest speed applied, a variation of graded composition in the range of 20 to 44 vol% of SiC was obtained. Moreover, such progressive concentration of particles was observed to be very homogeneous due to engulfment of particles (promoted by the high relative velocity between the solidification front and particles) and also as a consequence of elevated cooling rates developed in this case. Additional results showed that the matrix micro-structure is modified according to the SiC reinforcement content and cooling rates, which both depend on the centrifugal forces applied.

List of symbols

Subscripts

p	Particulate
Al	Aluminum
SiC	Silicon carbide
f	Fraction of particles
L	Liquid metal
r	Radial direction
c	Composite
m	Mold

Symbols

V_f	Volume fraction of particle
V_L^*	Initial particle volume fraction in melt
R	Solidification rate
d	Diameter of the particle
ρ_P	Density of the particle
ρ_L	Density of the liquid metal
η	Viscosity of melt
V_r	Radial velocity of the particle in melt
ω	Angular velocity
r	Radial coordinate
r_c	Radius of the reinforced zone
r_m	Radius of the mold
t	Solidification time
a, b	Empirical constants

1. Introduction

Metal matrix composites (MMCs) have great promise for high temperature, high strength and wear resistant applications. However, their brittleness has limited their use in load bearing applications. Functionally graded MMCs with a reinforcement concentration higher on the surface than in the interior offer new opportunities, as these materials will have high surface hardness as well as high resistance to crack growth towards the interior. Essentially, functionally graded materials (FGMs) are a relatively new form of composites having a continuous variation in composition along a certain direction. In the case of an Al/SiC_p FGM composite, the volume fraction of the reinforcement (SiC) changes gradually in the thickness direction inside the matrix (Al) to give a predetermined composition profile. Due to its novel character, FGMs are in the early stages of evolution and the basic experimental and theoretical studies on the mechanics of these materials must be done along with research in their processing [1, 2].

There are several investigators [3–8] which have done research on different areas related to centrifugally cast Al/SiC_p FGMs. Lajoye and Suéry [3, 4] presented a model to predict particle distribution in an Al-Si/SiC_p composite cylinder solidifying during centrifugal casting. The model developed takes into account the rate of displacement of the solidification front and the motion

*Author to whom all correspondence should be addressed.

of the particles in the centrifuged liquid. They found that the predictions were in good agreement with experimental observations. In addition, from the microstructural characterization of the graded composite obtained, they noticed changes in the dendritic structure of the Al phase due to SiC particle entrapment by the solidification front. Fukui and Watanabe [5] cast Al/SiC_p FGM rings by the centrifugal method. The rings had a variation of graded composition in the range of 0 to 43 vol% of SiC from the inner to the outer radial planes of the ring. The distribution of SiC particles in the Al alloy matrix was characterized by the optical microscopy of metallographic samples. The volume fractions of SiC were plotted as function of the specific radius and the SiC profiles were fitted with a polynomial function of third order. Furthermore, they evaluated the macroscopic residual stress in the Al/SiC_p FGM thick-walled ring by using a ring-cutting test and elasticity theory. Kang and Rohatgi [7] developed a numerical model of particle segregation during centrifugal casting of metal matrix composites considering thermal mechanical properties due to particles moving. These theoretical predictions were compared with Lajoye and Suéry's results [3] and good correlation was found. Moreover, they concluded that solidification time of the casting is dependent upon the speed of rotation of the mold, decreasing with an increase in speed. Liu *et al.* [8] presented a simple theoretical model to obtain gradient distribution of particles in centrifugal field. They found that the theoretical analysis is reasonable by comparing the results with SiC particle distribution in Al matrix composite produced by centrifugal casting.

As observed from the above literature review, centrifugal casting has been used to some extent to fabricate Al/SiC_p FGM, but the final product is limited to cylindrical shapes in the laboratory scale, such as tubes and rings with a graded composition along the radial direction. It is not easy to obtain from these tubes the appropriate flat specimens for testing mechanical strength related properties such as tensile testing and fracture analysis. Moreover, very few results were found in these works concerning the microstructural characterization (taking into account the parameters involved in centrifugal casting) of the Al/SiC_p FGM composites obtained. Thus, a centrifugal casting method is presented in this paper for processing Al/SiC_p FGM composite blocks of appropriated dimensions (aimed to test specimen fabrication), along with the corresponding microstructural characterization. Results are presented and discussed on SiC particles distribution, particles-solidification front interactions, matrix micro-structure, and porosity distribution in the castings as a function of the centrifugal forces applied.

2. Material and methods

The raw material used in these experimental castings was a homogeneous composite (A359 aluminum alloy matrix reinforced with 20-vol% silicon carbide particulate). It was obtained from Duralcan, Inc., with F3S.20S designation. The reinforcement particles were essentially single crystal alpha SiC, with a median particle size of 12.8 ± 4.2 μm. The matrix alloy is an Al-Si alloy whose composition is (by weight): 8.5–9.5% Si, 0.2% Fe, 0.2% Cu, 0.1% Mn, 0.5–0.7% Mg, 0.1% Zn, 0.2% Ti, 0.15% other elements, and the remain Al. Al forms a eutectic with 12.6 wt% Si at 577°C. The freezing range reported for commercial Al A359 alloys is 602–563°C [9]. The advantages of using this particular alloy are mainly due to the level of Si content present (8.5–9.5%) [10]. Silicon improves casting characteristics such as fluidity, hot tear resistance, and feeding. The optimum range of Si content for permanent mold casting is 7 to 9%. Furthermore, the amount of Si present in this alloy helps to reduce reactivity with SiC. Lloyd [11] found theoretically that the minimum level of Si is about 8-wt% to prevent Al_4C_3 formation.

Centrifuging is used in this case to process the functionally graded Al/SiC_p composite. The centrifugal force progressively increases the volume fraction of the SiC reinforcement within the liquid Al matrix along the radial direction, owing to the density difference between the two materials ($\rho_{Al} = 2300$ Kg/m^3 and $\rho_{SiC} = 3200$ Kg/m^3). A centrifuging machine was designed and built and its details are given in Fig. 1. The difference in this design from the commonly used centrifugal casting machines is that this device operated horizontally and pouring had to be done while the mold is stationary. Thus, centrifugal forces were not applied immediately as in the traditional casting methods since the mold takes some time to reach its casting speed. This delay had to be compensated by higher pouring and mold temperatures so that the desired particle segregation could be achieved. As a consequence, the cooling rate will be affected (the amount of heat to be extracted during solidification is higher) and this in turn will influence the microstructure of the composite.

In addition to the casting shapes that can be obtained with centrifuging, another major difference with respect to the traditional centrifugal casting is that in this latter case a unidirectional solidification front is produced from outside to inside diameter. In centrifuging, on the other hand, solidification fronts are produced from different directions of the mold. This can create some undesired effects on the final casting such as shrinkage porosity and a non-uniform distribution of the reinforcement particles. To avoid this, unidirectional solidification was enforced directly by water cooling of one side of the mold (at the outer circumference) with two perforated copper tubes located in the backstop of the centrifuging device and thus a chill plate was created to maintain rapid solidification of mold. Fig. 1 shows the details of the cooling device. The dimensions of the cast blocks produced are $50 \times 60 \times 100$ mm, weighing 900 grams each approximately.

Several parameters determine the microstructure and the distribution of particles inside the casting. These parameters are the size and initial concentration of particles, the centrifugal force, and the cooling rate, which last is controlled by: temperature of the mold, pouring temperature, cooling delay, cooling of the mold, cooling of the casting, and heat transfer between the mold and the melt. In these experiments all the parameters were fixed but the centrifugal acceleration. Thus, three castings were performed at 700 rpm, 1000 rpm, and 1300 rpm, which correspond to 100 g, 200 g, and 320 g

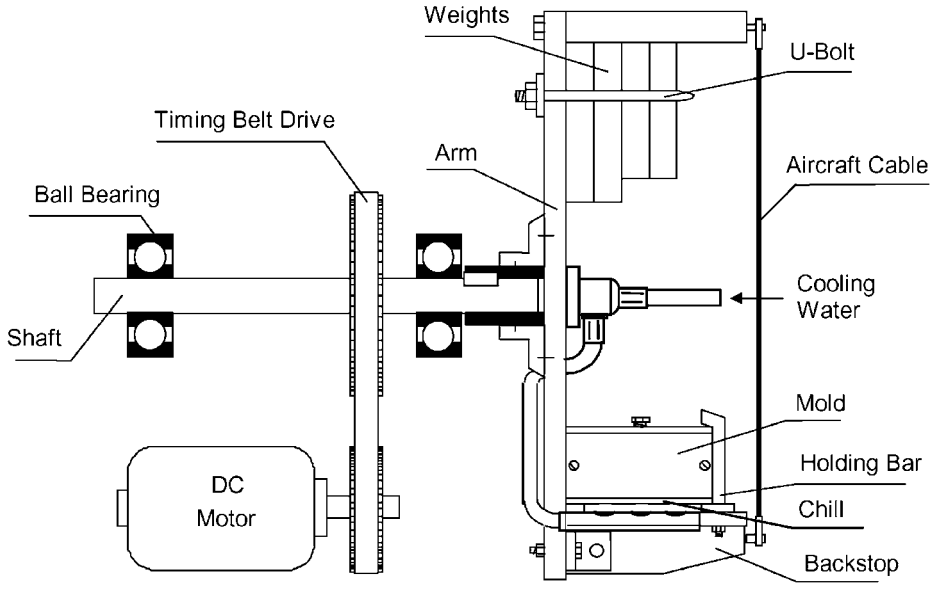

Figure 1 Centrifuge casting device.

centrifugal accelerations, respectively, with a fixed centrifuging radius of 178 mm. The values of the centrifugal accelerations are given in terms of g, the acceleration of gravity. The more influential casting conditions were kept constant: temperature of pouring at 750°C; temperature of the mold at 500°C; cooling delay of 10 s; cooling water flow of 10 liters/min, and weight of the composite at about 0.9 Kg. Reproducibility of the experiments was checked by repeating each casting at least twice.

Metallographic specimens of the centrifuged cast composite were obtained from different positions along the direction of variation of the SiC concentration. The samples were cut with the help of a diamond cut-off wheel. The metallographic specimens were ground using up to 600 grades of grinding papers and polished using 9, 6 and 3 μm diamond pastes.

3. Results and discussion

3.1. SiC particles distribution

One of the macroscopic pictures of the centrifugally cast FGM composite structure, which is obtained by the centrifugal acceleration of 1300 rpm, is shown in Fig. 2. In Fig. 3, the schematic representations of the structures were given for various centrifugal accelerations, namely, 700, 1000 and 1300 rpm. Microphotographs were taken at different positions of x that is chosen from the outer circumference of the cast block. The location of x is shown in Fig. 3. The volume fraction of silicon carbide as a function of position x was quantified using the point-counting method (ASTM E562) for each case and the results are plotted in Fig. 4a–c. The concentration of SiC particles increases in the direction of the centrifugal force for all the experiments, and concentrations as high as 44 vol% are obtained at the chill zone (region in the casting next to the chill plate where cooling rate is very high; the zone extends only a few millimeters) for the highest rotational speed of 1300 rpm. Moreover, a region completely denuded of particles was observed for all the experiments at the opposite side of the chill plate, this region becoming larger as the centrifugal force increased (see Fig. 3). The shape of the volume fraction profiles are in good agreement with the profiles obtained by experimental and numerical modeling by Lajoye and Suéry [3], Suéry and Lajoye [4], and Kang and Rohatgi [7].

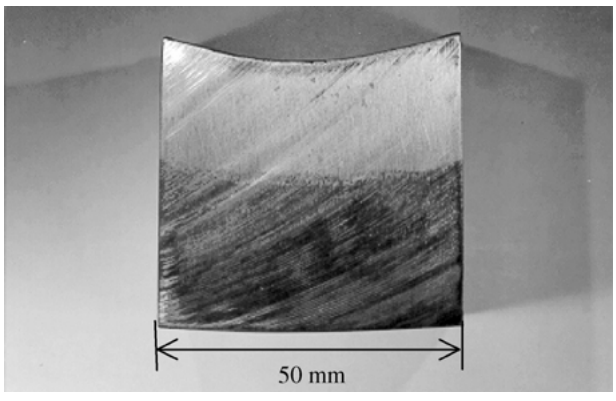

Figure 2 Photograph showing the cross section of the block cast at 1300 rpm.

For comparison purposes, theoretical predictions of the reinforcement distribution were done by using the analytical model developed by Liu *et al.* [8]. In this model, the particle distribution V_f in the FGM composite is expressed as

$$V_f = V_L^* \left(1 + \frac{V_r}{R}\right) \mathrm{e}^{-A\omega^2 t}, \qquad r_c \le r \le r_m \quad (1)$$

where V_L^* initial particle volume fraction in melt, R solidification rate, $A = \frac{d^2(\rho_p - \rho_L)}{18\eta^2}$, d diameter of the particle, ρ_p density of the particle, ρ_L density of the liquid metal, η viscosity of melt, V_r radial velocity of the particle in melt ($A\omega^2 r$), ω angular velocity, r radial coordinate, r_c radius of the reinforced zone (see Fig. 3), r_m radius of the mold (see Fig. 3), and t solidification time.

The assumptions made in this model are that solidification takes place unidirectionally with a planar front, the solidification rate R is constant, and there is no interaction between particles and solid/liquid interface during solidification. The predictions for the 700, 1000 and 1300-rpm castings are also plotted in Fig. 4a–c (with

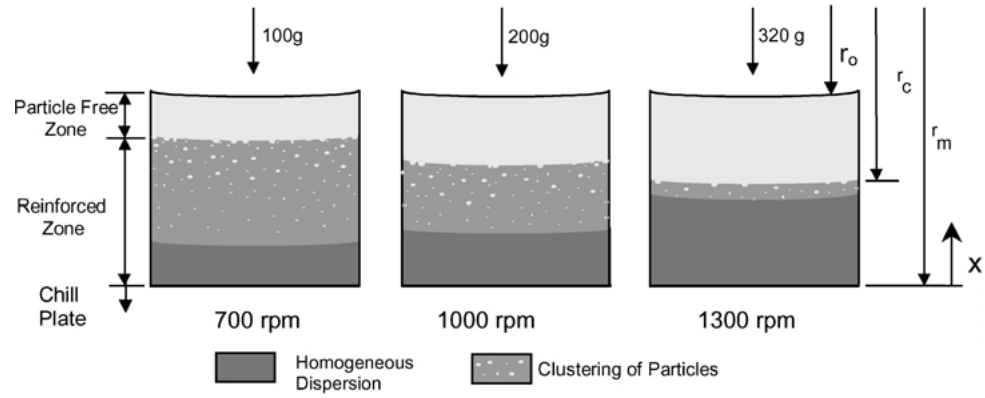

Figure 3 Schematic cross sections of the three castings.

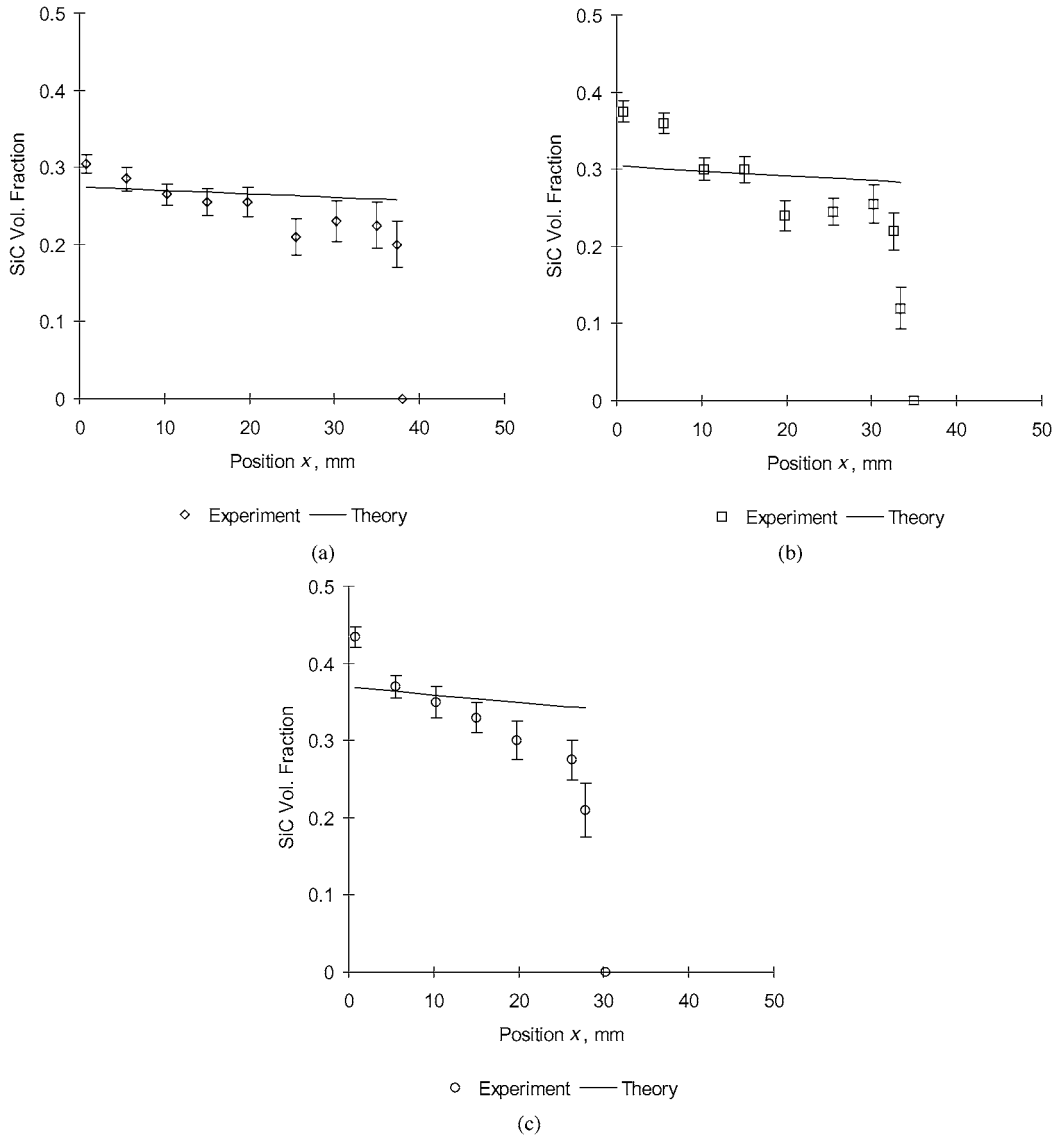

Figure 4 Experimental and predicted SiC distributions along the thickness of the castings, (a) 700, (b) 1000 and (c) 1300 rpm.

$x = r_m - r$), in which the following material parameters were used: $V_L^* = 0.2$, $d = 12.8$ μm, $\rho_L = 2300$ kg/m^3, $\rho_P = 3200$ kg/m^3, $\eta = 0.0015$ N-s/m^2 (at about 750°C, [13]), $r_m = 0.20$ m, and $r_c = 0.162$, 0.166, and 0.172 m for the 700-rpm, 1000-rpm, and 1300-rpm cases, respectively.

The solidification rates calculated from critical thickness ($r_m - r_c$) measurements in the three castings are $R = 0.014$, 0.02, and 0.02 m/s for the 700-rpm, 1000-rpm and 1300-rpm castings, respectively. As observed, the predicted volume fraction values show little variation with position; the measured values show a much steeper slope. This was expected since the model presumes that solidification begins right from the application of the centrifugal force. In the present experiments the solidification starts a few seconds after the

centrifugal field has begun to operate, thus allowing more time for the reinforcing particles to take on a more slanted profile. Furthermore, the model does not take into account the amount of superheat in the melt that has to be extracted or the heat transfer conditions of the mold wall, which delays even more the onset of solidification. In addition, the assumptions of constant solidification rate and no interactions between particles and solid-liquid interface are not always valid since solidification rate changes with the distance from the chill [14]. Finally, some rejection of particles, which is detailed in the following section, by the solidifying melt is noted in the present experiments even at relatively high speeds. These factors also have an effect on the final distribution of particles.

3.2. Particles-solidification front interactions

The concentration of particles was very homogeneous for the 1300-rpm casting, whereas some clustering of particles was detected in the 700-rpm and 1000-rpm castings. These can be seen in Fig. 5, which were taken at various positions of x in the reinforced region (see Fig. 3 for the location of x). In the chill zone, the distribution of particles was uniform with no regions devoid of particles in the three castings. This regular concentration of particles extended about 15 mm from chill plate for the 700-rpm and 1000-rpm castings (see Fig. 5a, b, d and e) while in the 1300-rpm casting the uniform dispersion extended to almost the entire reinforced region (see Fig. 5g–i). Beyond the chill zone, particle free

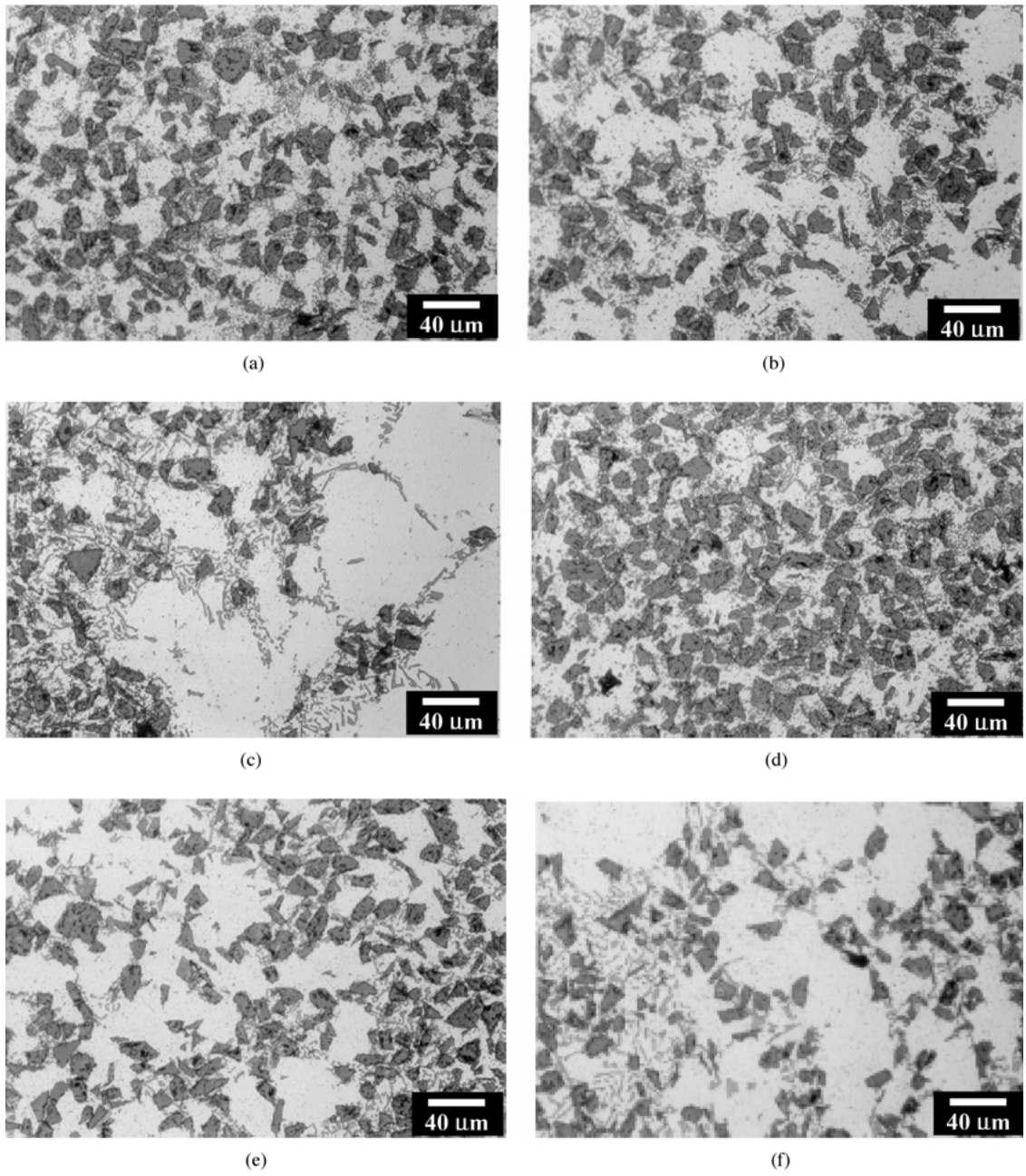

Figure 5 Optical micrographs showing matrix microstructure and SiC particles distribution. (a) 700 rpm, 0.79 mm from chill plate, 0.32 vol. fraction. (b) 700 rpm, 15.08 mm from chill plate, 0.23 vol. fraction. (c) 700 rpm, 37.31 mm from chill plate, 0.18 vol. fraction. (d) 1000 rpm, 0.79 mm from chill plate, 0.39 vol. fraction. (e) 1000 rpm, 15.08 mm from chill plate, 0.30 vol. fraction. (f) 1000 rpm, 30.16 mm from chill plate, 0.24 vol. fraction. (g) 1300 rpm, 0.79 mm from chill plate, 0.45 vol. fraction. (h) 1300 rpm, 10.32 mm from chill plate, 0.35 vol. fraction. (i) 1300 rpm, 26.19 mm from chill plate, 0.23 vol. fraction. (*Continued*)

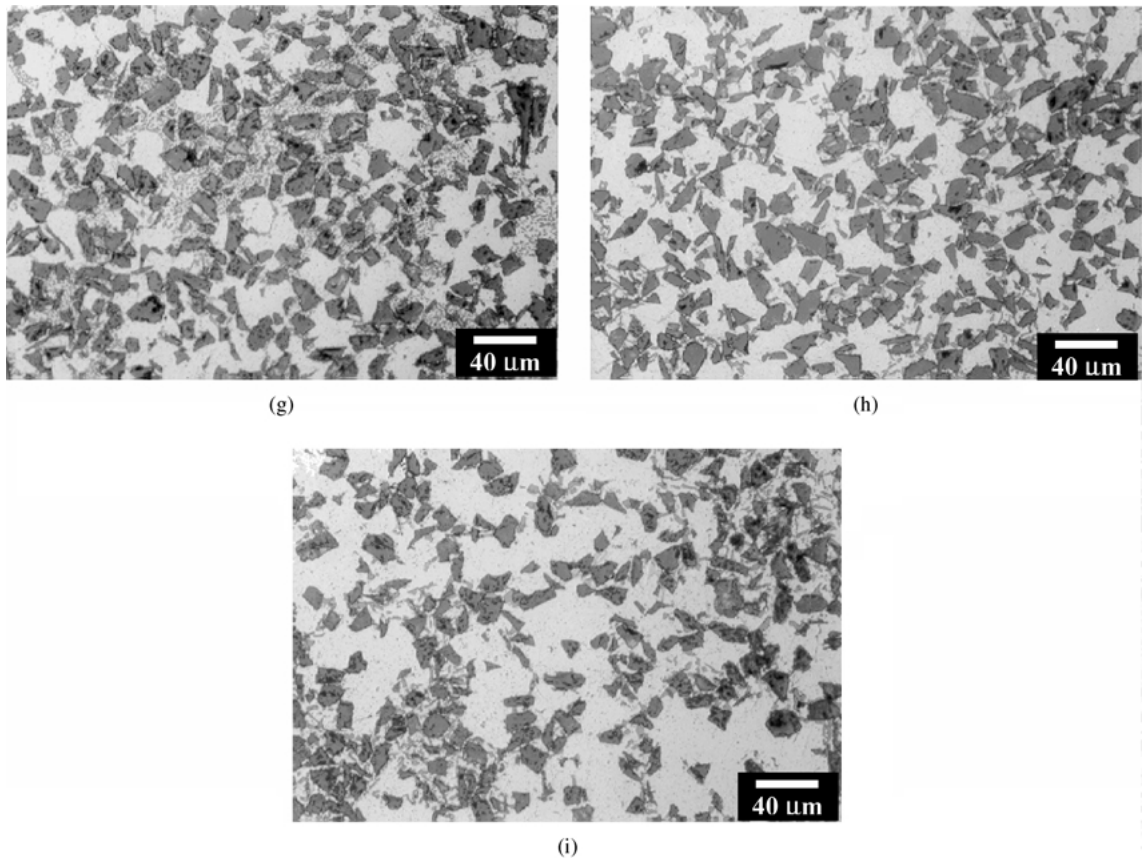

Figure 5 (*Continued*).

islands (due to the clustering of particles) of increasing sizes at increasing distances from the chill plate were observed for the 700 and 1000-rpm castings, the size being smaller in the latter casting. Thus, for instance, the 1000-rpm casting displays particle free islands up to 100 μm in size (see Fig. 5f) whereas in the 700-rpm casting islands void of particles up to 120 μm in size were observed (see Fig. 5c). The 1300-rpm casting also shows particle free islands, but these are restricted to a narrow region (see zone with clustering of particles in Fig. 3) and they are smaller in size (about 80 μm, see Fig. 5i). Despite the fact that some agglomeration of particles is observed in the three castings, the overall macroscopic distribution is quite homogeneous given that particle free zones up to 200 μm in size have been reported in chill casting experiments without centrifugal force by Lloyd [11] and Pasciak [15] with similar Al/SiC_p systems.

The mechanisms for rejection and clustering of SiC particles in solidifying Al/SiC_p melts are well known for static castings [11, 14, 16]. It has been established that the interaction between solidification fronts and particles as well as the size of the micro-constituents of the matrix structure are responsible for the final distribution of particles in the cast composite. Generally, at high solidification rates the cell size or dendrite spacing is smaller than the particle size and the distribution of particles in the solidified composite remains the same as in the liquid state. There is engulfment rather than rejection of particles due to the interaction of solid-liquid interface in the high velocity. When the dendrite growth occurs at lower cooling rates, and if the cells and the particles are comparable in size, then the particles are geometrically trapped in interdendrite regions, while for further dendrite growth and increasing cell sizes, particle agglomeration is enhanced due to the more particle pushing and less geometrical trapping.

The unifying particle pushing theory, which describes interactions between solidification fronts and unrestrained particles in static castings is not fully developed yet [16], but there are several experimental and theoretical studies aimed at predicting particle pushing/entrapment. The various analytical and empirical models developed so far make predictions according to thermodynamic and kinetic interpretations of particle pushing, and most of them use the concept of critical solidification front velocity above which particles are engulfed and below which particles are rejected by the solidification front. Rohatgi *et al.* [16] presented some results on particle-front interactions in Al/SiC_p composites based on current theoretical models of the phenomenon. From these models, it is observed that the predicted values of critical velocity are very low except in the model proposed by Stefanescu *et al.* [17]. Wu *et al.* [14] supported the Stefanescu *et al.* model based on their experimental and numerical findings on calculation of critical velocities in the Al/SiC_p system.

In centrifugal castings where high centrifugal forces are involved, the particles are restricted to move in the direction of the centrifugal force with increasing radial speeds at increasing angular velocities. The solidification front, on the other hand, moves in the opposite direction with a variable speed toward the inner circumference of the casting. Moreover, it has been experimentally observed in the present investigation (see Fig. 6), and also reported by Suéry and Lajoye [4],

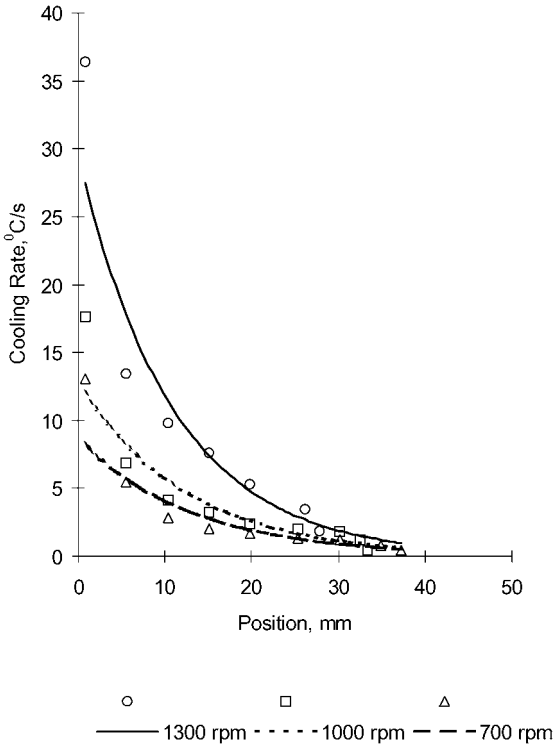

Figure 6 Predicted cooling rates along the thickness of the castings.

Vaidyanathan [18], and Yeh and Jong [19], that cooling rate is enhanced with increasing casting speeds because of better heat transfer at the chill plate (high centrifugal forces produce a tight contact between the mold wall and the melt) and also due to the presence of thermally insulating SiC particles (higher SiC contents reduce the amount of heat to be removed and this causes an increase in the solidification rate). The high cooling rate gives rise to a much finer cast microstructure. Accordingly, the conditions seem favorable for the Al/SiC_p composites cast at high centrifugal accelerations to obtain a very uniform distribution of particles. In the first place, the particles are less likely to be rejected by the solidification front due to the high relative velocity between the solid-liquid interface and the particles, this velocity even surpassing the critical front velocity given by Stefanescu *et al.* [17] for pushing. Secondly, a finer microstructure (product of high cooling rates, as mentioned) produces a more even SiC distribution due to restricted cell growth, which causes the reinforcement particles to be pushed shorter distances. The above conditions were realized in the 1300-rpm casting in which a highly homogeneous graded distribution of SiC particles was observed. On the contrary, for the lower speed castings, 700 and 1000 rpm, small agglomerations of particles were present at positions far from the chill, as has been previously mentioned. In these cases, and according to Fig. 6, lower cooling rates and less restrained dendrite growth at lower speeds are responsible for more pushing of the SiC particles to the interdendritic sites.

The cooling rates in Fig. 6 were computed from cell size measurements obtained from the micrographs. Cell size d and cooling rate R are related according to [20]:

$$d R^a = b, \tag{2}$$

where a and b are empirical constants. Values of $a = 0.36$ and $b = 50$, corresponding to an Al A356/SiC_p composite [11], were used in the calculations of data in Fig. 6. The Al A356 alloy is very similar to the Al A359 alloy. The freezing range of the Al A356 is 615 and 563°C whereas for the Al A359, it is 602 and 563°C. The particle size used in the Al A356/SiC_p composite is 10 μm compared to 13 μm in the present composite. In addition, a is typically in the range 0.34–0.39 for monolithic alloys and it has been observed by Lloyd [11] that the presence of reinforcing particles does not significantly affect the solidification cell size at cooling rates below 100°C/s.

3.3. Dendrite structure modification

Spatial variations of the matrix structure are seen in all of the centrifuge Al/SiC_p castings. In the reinforced region, the dendritic matrix structure appears to be inhibited by the presence of the SiC particles and the effect of high centrifugal forces. Very fine equiaxed cells are observed in the chill zone (see Fig. 5a, d, g), becoming coarser as one moves toward the transition to the particle free region (see Fig. 5b, e, h). After this transition, in the unreinforced region, the dendritic structure appears to be partially modified, consisting of equiaxed dendrites increasing in size as the distance from the chill zone is increased (see Fig. 5c, f, and i).

The altered matrix structure obtained here is the result of a combination of various phenomena taking place during centrifugal solidification of the composite. The first is the inherent effect of SiC particles in refining the microstructure. Rohatgi *et al.* [16] and Rohatgi and Asthana [21] mentioned that the structure morphology is changed because solidification takes place in very restricted zones in the interstices between particles, and this effect is magnified by high volume fractions of particles.

Second, the presence of high centrifugal forces also has a major effect on the final microstructure as has been suggested by Vaidyanathan [18]. He performed an analysis on the effect of high centrifugal accelerations (ranging from 100 g to 800 g) during solidification of an Al A356 alloy. He argued that the large centrifugal forces cause the breaking of dendrites due to a column or a cantilever loading state and to a lesser degree by the shearing action of the liquid at the solid-liquid interface. This breaking contributes to an increase in the fine equiaxed zone, as it is observed in the present work.

Although the experiments performed by Vaidyanathan [18] were done with unreinforced materials only, it seems reasonable to assume that the above mentioned mechanical effects are magnified with the presence of the reinforcing particles. In fact, particles heavier than the aluminum melt can load severely the branches of the primary and secondary dendrites amplifying their susceptibility to failure, while the melt becomes more viscous at increasing contents of particles thus intensifying the friction effect of the liquid on the solid-liquid interface. In summary, we conclude that the matrix structure in the reinforced region is refined due to the following effects: solidification taking place rapidly and in very

restricted spaces; and breaking of dendrites by the combined loading action of high centrifugal forces and accelerated particles.

3.4. Eutectic modification

There is also a variation of the eutectic structure along the direction of the centrifugal force in the castings. This spatial variation consists of various degrees of quench modification going from a fully modified eutectic structure at the chill zone to partially modified at the transition between the reinforced and particle free zones. In the unreinforced part, when going from the transition region to the inner circumference of the casting, the eutectic went from a partially modified structure to an unmodified structure. All these changes were observed under the microscope, where a quench-modified fibrous eutectic silicon structure can be seen at the chill zone (Fig. 5a, d, g); a mainly eutectic flake silicon (with some angular silicon) is present at the transition (Fig. 5c); and a massive faceted eutectic silicon structure is observed at the opposite side of the chill zone. Also, it is noted in general that Si nucleates and grows on SiC particles and in many cases, a considerable number of SiC particles are joined together by the Si phase.

3.5. Casting defects

Microscopic porosity was observed in specific zones of the reinforced and unreinforced regions of the FGM castings. Porosities no bigger than 100 μm in size were present in all castings in the particle free region at very close distances from the free surface. This zone comprises a thin skin, which has solidified before the rest of the unreinforced region due to cooling by air convection and heat irradiation. As a result, most of these porosities have formed by solidification shrinkage as evidenced by their irregular shapes. Such porosities represent no major problem for application purposes since this skin can be machined away. On the other hand, in the reinforced region, a few microporosities (see Fig. 7) up to 50 μm in size are detected in the castings at 700, 1000, and 1300 rpm. The casting at 1300 rpm presented the highest incidence of porosities with an estimated pore volume fraction of less than 2% for this casting (measuring the area fraction of porosities in a sample area of 600 mm^2). The origin of these microporosities, as indicated by microscopic analysis, is mainly solidification shrinkage, although some gas porosities are observed perhaps due to hydrogen pickup during the melting and/or the stirring processes. In general, shrinkage microporosity occurs because in most alloy casting processes the solidification morphology is dendritic. Therefore, flow of fluid to feed shrinkage occurs through conduits between dendrite branches [20]. By extending this idea to particulate composites, where the reinforcement particles segregate into these interdendritic regions, the feeding of solidification shrinkage is less effective due to partial blocking of the conduits by the particles and also due to increased viscosity of the melt with particles. Consequently, the higher the volume fraction of SiC particles the higher the resistance of interdendritic fluid flow to feed solidification shrinkage. These phenomena explain why in the present experiments the 1300-rpm casting contained more microporosity than the others did. At 1300 rpm, as higher density of particles was achieved, it became harder for the melt to flow between the branches of the dendrites, and thus shrinkage microporosity was formed even in the presence of high centrifugal pressures and rapid and progressive solidification.

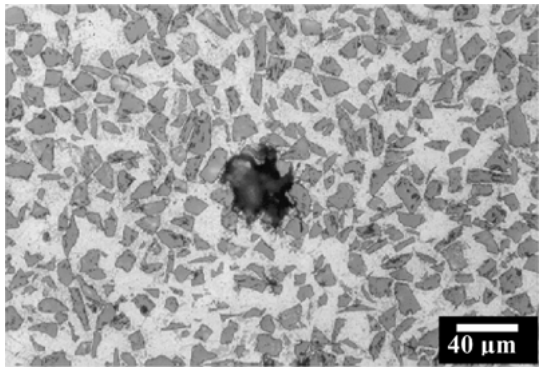

Figure 7 Microporosity produced by solidification shrinkage.

4. Conclusions

Centrifuge casting was presented as an alternative method to produce Al/SiC$_p$ FGM composite rectangular blocks, from which appropriate specimens can be obtained for tensile and fracture testing. In following works, the effect of the continuous compositional variation on fracture properties of this material will be described.

The volume fraction profiles varied as the centrifugal force was applied, and concentrations as high as 44 vol% were obtained at the outer circumference for the maximum angular speed. This can have potential applications in high temperature and wear resistance environments.

For the casting conditions used in the 1300-rpm casting the progressive concentration of particles was homogeneous due in part to engulfment promoted by the high relative velocity between the solidification front and the particles, and also due to the elevated cooling rates developed in this case. On the contrary, for the 700-rpm and 100-rpm experiments, agglomeration of particles was observed because of the lower intensity of the above parameters.

The matrix structure is modified in the reinforced region as a consequence of solidification taking place rapidly and in very restricted spaces and also due to breaking of dendrites by the combined loading action of accelerated particles and loaded dendrites. Quench modification of the eutectic structure was observed, going from a fully modified structure at the chill to an unmodified structure at the opposite side of the casting.

Microporosity was detected in the castings at three angular speeds, being more pronounced in the 1300-rpm case, contrary to expectations. It is suggested that higher concentrations of particles in this case decrease the ability of interdendritic fluid flow to feed solidification shrinkage.

References

1. F. ERDOGAN, *Composites Engineering* **5** (1995) 753.
2. R. WATANABE, *MRS Bulletin* **20**(1) (1995) 32.
3. L. LAJOYE and M. SUÉRY, in "Cast Reinforced Metal Composites," edited by S. G. Fishman and A. K. Dhingara (ASM International, 1988) p. 15.
4. M. SUÉRY and L. LAJOYE, in "Solidification of Metal Matrix Composites," edited by P. Rohatgi (The Minerals, Metals & Materials Society, 1990) p. 171.
5. Y. FUKUI and Y. WATANABE, *Metall. and Mater. Trans.* A **27A** (1996) 4145.
6. Y. FUKUI, N. YAMANAKA and Y. ENOKIDA, *Composites* B **28B** (1997) 37.
7. C. G. KANG and P. ROHATGI, *Metall. and Mater. Trans.* B **27B** (1996) 277.
8. Q. LIU, Y. JIAO, Y. YANG and Z. HU, *ibid.* **27B** (1996) 1025.
9. CINDAS, "Structural Alloys Handbook" (Purdue University, 1994).
10. E. L. ROOY, "ASM Handbook," 10th ed., Vol. 15 (1998).
11. D. J. LLOYD, *Composites Science and Technology* **35** (1989) 159.
12. J. A. SNIDE, L. G. BATES, F. A. ASHDOWN and J. R. MYERS, *J. Composite Materials.* **2**(4) (1968) 509.
13. R. N. LYON (ed.) "Liquid-Metals Handbook" (1954).
14. Y. WU, H. LIU and E. J. LAVERNIA, *Acta Metall. Mater.* **42** (1994) 825.
15. K. J. PASCIAK, M.Sc. thesis, University of Wisconsin-Milwaukee, 1991.
16. P. ROHATGI, R. ASTHANA and F. YARANDI, in "Solidification of Metal Matrix Composites," edited by P. Rohatgi (The Minerals, Metals & Materials Society, 1990) p. 51.
17. D. M. STEFANESCU, B. K. DHINDAW, S. A. KACAR and A. MOITRA, *Metall. Trans.* A **19A** (1988) 2847.
18. CH. VAIDYANATHAN, Ph.D. dissertation, University of Wisconsin-Madison, 1994.
19. J. W. YEH and S. H. JONG, *Metall. and Mater. Trans.* A **25A** (1994) 643.
20. M. C. FLEMINGS, "Solidification Processing" (McGraw-Hill, New York, 1974) p. 148.
21. P. ROHATGI and R. ASTHANA, *JOM* **43**(5) (1991) 35.

Received 9 April
and accepted 6 December 2001